HHS Public Access

Author manuscript

ACS Nano. Author manuscript; available in PMC 2021 April 30.

Published in final edited form as:

ACS Nano. 2020 March 24; 14(3): 2994–3003. doi:10.1021/acsnano.9b07865.

Antibody Response against Cowpea Mosaic Viral Nanoparticles Improves *In Situ* Vaccine Efficacy in Ovarian Cancer

Sourabh Shukla, **Chao Wang**, **Veronique Beiss**

Department of NanoEngineering, University of California–San Diego, La Jolla, California 92039, United States

Nicole F. Steinmetz

Department of NanoEngineering, Department of Bioengineering, Department of Radiology, Moores Cancer Center, and Center for Nano-ImmunoEngineering, University of California–San Diego, La Jolla, California 92039, United States

Abstract

Cancer immunotherapies are designed to facilitate recognition and elimination of transformed cells by the immune system. We have established the immunotherapeutic efficacy of the plant virus cowpea mosaic virus (CPMV) as an *in situ* vaccine in several syngeneic tumor mouse models as well as in companion dogs with metastatic melanoma. Intratumoral injection of CPMV modulates the local tumor microenvironment to relieve immunosuppression and potentiate antitumor immunity. The viral nucleocapsid that drives this antitumor immunity, however, also is a potent immunogen itself, and thus immune response in the form of anti-CPMV antibodies is expected during the treatment based on repeat administrations. Moreover, being part of the food chain, pre-existing antibodies to plant viruses may be prevalent. The presence of such pre-existing anti-CPMV immunity could potentially impact immunotherapeutic efficacy of the *in situ* vaccine and could have translational implications. To address such concerns, this study evaluated the efficacy of CPMV *in situ* vaccine in the presence of pre-existing antibodies in a syngeneic mouse model of ovarian cancer. Our results indicate that prior exposure to CPMV had no negative impact on the efficacy of CPMV *in situ* vaccine. Strikingly, an improved efficacy of CPMV *in situ* vaccine was observed. This study therefore presents an important milestone in the translational development of plant viral-based *in situ* vaccines and alleviates concerns about the presence of anti-CPMV antibodies, which are developed during the course of treatment but have no impact on immunotherapeutic efficacy.

Graphical Abstract

Corresponding Author: **Nicole F. Steinmetz** – Department of NanoEngineering, Department of Bioengineering, Department of Radiology, Moores Cancer Center, and Center for Nano-ImmunoEngineering, University of California–San Diego, La Jolla, California 92039, United States; nsteinmetz@ucsd.edu.

The authors declare no competing financial interest.

Complete contact information is available at: https://pubs.acs.org/10.1021/acsnano.9b07865

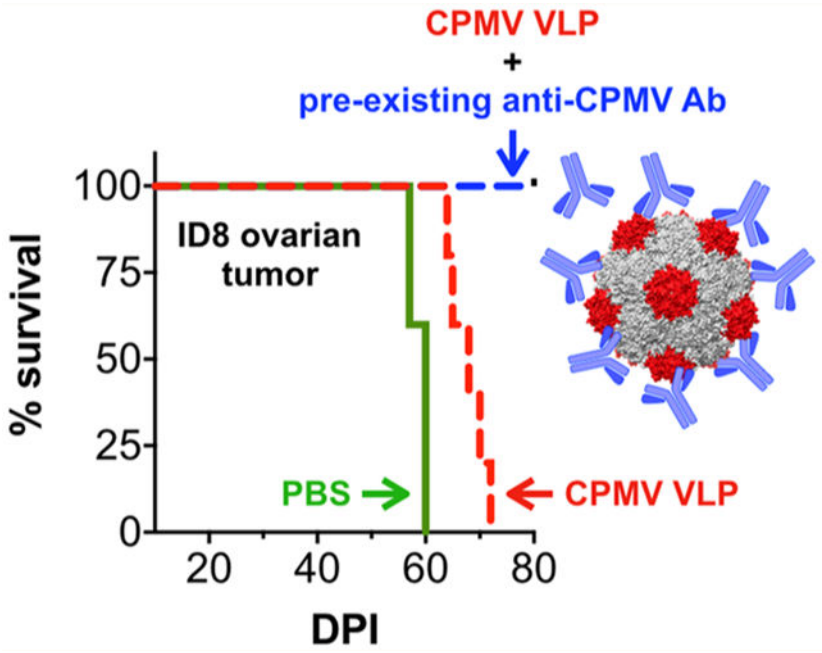

Keywords

plant viruses; CPMV; in situ vaccine; cancer immunotherapy; ovarian cancer; antiviral antibodies

Cancer immunotherapies are designed to enable recognition and elimination of transformed cancer cells by the immune system.[1] Aggressively growing tumors create a highly immunosuppressive tumor microenvironment (TME) that depletes antitumor responses and promotes tumor progression.[2] Therefore, localized cancer immunotherapies such as *in situ* vaccines[3,4] and oncolytic viruses[5] that facilitate reversal of immune suppression in the TME leading to a systemic antitumor response are particularly promising interventions.

The plant-derived cowpea mosaic virus (CPMV) and its nucleic-acid-free virus-like particle (VLP or eCPMV) have been established as highly potent *in situ* vaccines.[6,7] The proteinaceous architecture of CPMV or its VLP imparts exceptional immunostimulatory properties capable of relieving local immune suppression and orchestrating a systemic antitumor immune response. Specifically, we have demonstrated that *in situ* vaccination with CPMV/VLPs can overturn the immunosuppressive TME and instigate a potent local and systemic antitumor immune response in syngeneic mice tumor models of melanoma,[6,7] breast,[6] ovarian,[8] and colon cancer,[6] and glioma[9] and companion dogs with oral melanoma.[10] The CPMV *in situ* vaccine effectively obstructed tumor progression and improved disease-free survival. Our data across these tumor models have indicated that the intratumoral administration of CPMV leads to a cascade of events including infiltration and activation of innate immune cells, secretion of pro-inflammatory cytokines including IL-6, TNF-α, and IFN-γ, reduction in pro-tumor cytokines IL-10 and TGF-β, and buildup of natural killer (NK) cells, as well as antitumor neutrophils and macrophages through recruitment or repolarization.[6–8] Subsequently cancer cell death mediated through innate immune cells exposes tumor-associated antigens to recruited professional antigen-presenting

cells, which then prime the adaptive arm of antitumor response and immune memory, therefore protecting against outgrowth of metastatic disease and/or recurrence.

Unlike oncolytic viruses, which selectively infect, replicate in, and lyse tumor cells to debulk tumors and initiate the cancer immune cycle, plant viruses are nonreplicative in mammalian cells. Therefore, the immunomodulation of the TME by CPMV/VLP *in situ* vaccine is driven by its immunostimulatory multivalent nucleoprotein architecture.[6] The innate immune system in mammals has evolved to recognize and respond to pathogens through an array of pattern recognizing receptors (PRRs) and Toll-like receptors (TLRs).[11] It is the activation of PRRs and TLRs by CPMV that leads to the onset of the antitumor response. However, the inherent immunogenicity of CPMV may also lead to the development of an anti-CPMV immune response, manifested as anti-CPMV antibodies and T cells. In fact, such an immune response plays a key role in reducing microbial burden and protection against viral antigens.[12] The CPMV *in situ* vaccine is typically administered in multiple doses, which may prime anti-CPMV immune responses. Moreover, as part of the natural food chain, prior exposure to plant viruses is common, and antibodies to plant viruses have been reported (although there are no reports analyzing the prevalence of CPMV antibodies in the human population).[13,14]

Anti-CPMV antibodies, pre-existing or as a result of repeated treatment, could have significant implications for the efficacy as well as safety of the CPMV immunotherapy. Increased clearance rates may reduce the effective therapeutic dose available in the tumor. The suboptimal dosing could therefore diminish efficacy of CPMV immunotherapy. Additionally, patients harboring prior immunity to CPMV could show adverse reaction/hypersensitivity to CPMV immunotherapy and would need to be precluded from the treatment. Such concerns regarding safety and efficacy could have significant translational implications and therefore require investigation. Therefore, we specifically asked the following questions: (1) Does the CPMV *in situ* vaccine induce an anti-CPMV antibody response? and (2) if yes, does the presence of pre-existing antibodies mitigate the efficacy of CPMV *in situ* vaccine?

RESULTS AND DISCUSSION

Production and Bioconjugation of CPMV/eCPMV.

CPMV was propagated in black-eyed pea plants (*Vigna unguiculata*) and purified using protocols described previously[15] with yields of 50 mg/100 g infected leaves. eCPMV particles was produced by coexpression of the precursor to the large (L) and small (S) coat proteins (VP60) and the viral proteinase (24K) in *Nicotiana benthamiana* leaves with similar yields; the methods are as previously described.[16] Particle integrity following purification was determined using size exclusion chromatography (Figure 1A). Both CPMV and eCPMV show the characteristic elution profiles (and elute at 10–15 mL from a Superose 6 column) with the characteristic 260:280 ratios of 1.7 and 0.7 for CPMV and eCPMV, respectively. Next, *N*-hydroxysuccinimide (NHS) chemistry was used to synthesize fluorescent and PEGylated particles (Cy5 was chosen to enable tracking of the particles, and PEG was chosen to reduce immune cell and antibody interactions).

The NHS ester of Sulfo-Cy5 (NHS-Sulfo-Cy5) and PEG2000 (NHS-PEG2000) were conjugated to CPMV and eCPMV *via* the solvent-exposed Lys residues to produce CPMV-Cy5, eCPMV-Cy5, PEG-eCPMV, and PEG-eCPMV-Cy5 particles (Figure 1B).[17] Particle concentrations and dye numbers were determined through UV–vis analysis using the extinction coefficients ε_{CPMV} = 8.1 mL mg^{-1} cm^{-1} at 260 nm and ε_{eCPMV} = 1.28 mL mg^{-1} cm^{-1} at 280 nm and molar extinction coefficient $\varepsilon_{sulfo\text{-}Cy5}$ = 271 000 L mol^{-1} cm^{-1} at 647 nm. Using a 5000 molar excess of NHS-sulfo-Cy5/(e)CPMV, 80 and 88 dyes were conjugated on CPMV and eCPMV particles, respectively.

PEGylation was carried out using eCPMV or eCPMV-Cy5 particles using a 5000 molar excess of PEG2000 to yield PEG-eCPMV and PEG-eCPMV-Cy5 particles. Denaturing SDS-PAGE was used to confirm covalent dye (fluorescent light) and PEG conjugation (white light poststaining) (Figure 1C). Unmodified CPMV (and eCPMV) showed two characteristic bands corresponding to the ~24 kDa small coat protein (S-CP) subunit and the ~42 kDa large coat protein subunit (L-CP) (lanes 1, 3, and 5). Fluorescence imaging of the gels confirmed Cy5 conjugation to both S-CP and L-CP (lanes 2, 6, and 7); the presence of additional higher molecular weight bands in the stained gel indicated successful PEGylation of the S and L proteins; however more distinct, sharp bands were observed above the S-CP (lanes 4 and 7). Quantification of the band intensity by densitometry analysis of the stained gel (Fiji software) indicated ~50% of S-CP in PEG-eCPMV (lane 4) modified with PEG; a similar % of PEGylation is expected on the L-CP, therefore totaling ~60 PEG chains per eCPMV. Similar quantification of the PEG-eCPMV-Cy5 (lane 7) indicated ~30% of S-CP modified with PEG along with L-CP, suggesting ~36 PEG chains per eCPMV-Cy5. PEG-eCPMV-Cy5 particles were prepared by reacting NHS-PEG with purified eCPMV-Cy5 particles. Since both NHS-Cy5 and NHS-PEG utilize lysine residues on the viral capsids, PEGylation of eCPMV-Cy5 is less efficient than that of eCPMV.

Immunogenicity of CPMV/eCPMV.

We determined whether repeat administration of CPMV particles as *in situ* vaccine would lead to generation of anti-CPMV antibodies in mice. All animal experiments were carried out in accordance with University of California San Diego's Institutional Animal Care and Use Committee (IACUC). Female C57BL6 mice (7 weeks old, n = 5) received six weekly intraperitoneal (i.p.) injections of CPMV, eCPMV, or PEG-eCPMV (100 μg/200 μL PBS) to mimic the CPMV *in situ* vaccine schedule established for ID8 ovarian cancers in our lab (Figure 2A, SET 1).[18] Blood sera were collected and analyzed for anti-CPMV antibodies and isotypes prior to first injection (naive sera) and a week from the last injection (postimmunotherapy sera, day 49).

A second set of mice was used to evaluate and compare the anti-CPMV immune response in mice with prior CPMV exposure (Figure 2B, SET 2). Here, mice were immunized with CPMV *via* two subcutaneous (s.c.) injections (50 μg CPMV/50 μL PBS) 2 weeks apart prior to commencement of i.p. injections with CPMV, eCPMV, or PEG-eCPMV as outlined in Figure 2A. Blood sera were collected from naive mice, following the s.c. immunizations (day −3 sera) and a week from the completion of immunotherapy (day 49 sera). Sera collected from these groups of mice were first evaluated for the presence of anti-CPMV

antibodies by ELISAs using plates coated with CPMV (Figure 2C,D). Naive sera from both sets were, as expected, negative for anti-CPMV antibodies (naive sera), whereas all other mice that received CPMV, eCPMV, or PEG-CPMV as s.c. or i.p. were positive for anti-CPMV antibodies (d49 sera). Our data indicate that the repeat i.p. treatment using (e)CPMV as an *in situ* vaccine leads to a CPMV-specific immune response, which is what one would expect. Of course, mice that were preimmunized with CPMV to mimic antibody prevalence had overall higher titers following i.p. *in situ* vaccination; this can be explained by the fact that the i.p. treatment acts as a boost to the initial prime dose of CPMV.

The 4-fold higher titers indicate enhanced immunogenicity of CPMV (d49 sera end point titer 1:2 000 000) over eCPMV and PEG-eCPMV (d49 end point titer 1:500 000). These differences in the immunogenicity of CPMV *vs* eCPMV can be attributed to the encapsidated RNA or lack therefore. RNA acts as an agonist for TLR7/8 and thus functions as adjuvant, leading to more robust immune stimulation when CPMV is used.[8,19–22] Lastly, a comparison of anti-CPMV antibody isotypes from the pooled day −3 sera (s.c. CPMV immunizations) and day 49 sera following CPMV i.p. administrations from naive (SET 1) and pre-exposed mice (SET 2) indicated prevalence of anti-CPMV IgGs with a dominance of IgG2b isotype (Figure 2E). Similarly, day 49 sera following eCPMV and PEG-eCPMV i.p. treatment was dominated by anti-CPMV IgG2b isotypes (data not shown). We have previously shown that CPMV elicits a Th1-biased immune response,[23,24] in agreement with the IgG2b dominant subtype.

These results confirmed that immunotherapy with CPMV/eCPMV with or without prior exposure to CPMV leads to an anti-CPMV immune response that is manifested as anti-CPMV antibodies.

Impact of Pre-existing Antibodies on CPMV *In Situ* Vaccine Efficacy.

Given the strong humoral immune response generated against CPMV, we next compared the efficacy of the *in situ* vaccine in CPMV pre-exposed mice. Thus, two sets of mice, one CPMV-naive and the other CPMV-pre-exposed (*via* subcutaneous immunizations, as described above), were challenged i.p. using the syngeneic ID8-Defb29/Vegf-a[25] ovarian cancer cells (2 million cells/mouse) (Figure 3A,B). Starting at 7 days post tumor inoculation, mice were treated with six weekly doses of CPMV immunotherapy (100 μg of CPMV in 200 μL of PBS) or PBS *via* i.p. injections. Tumor progression was monitored by measuring gains in mouse circumference (Figure 3C) and body weight (Figure 3D) resulting from increased tumor burden and development of ascites. Mice were euthanized when the circumference and weights reached 10 cm or 30 g, respectively.

PBS-treated mice reached the sacrifice criteria within 52 days (Figure 3E). The CPMV *in situ* vaccine was demonstrated to be effective in both naive and CPMV-pre-exposed mice; interestingly the *in situ* vaccination proved to be more effective in mice pre-exposed to CPMV. Thus, there appears to be no concern about neutralizing antibodies; rather the presence of antibodies enhanced the efficacy of the CPMV *in situ* vaccine (see below for further discussion). The CPMV-naive group had fewer survivors compared to the pre-exposed mice. There were significant differences in the survival between the untreated and treated groups ($p = 0.0002$ and $p < 0.0001$), and the *in situ* vaccine also resulted in a

significantly improved survival comparing CPMV-pre-exposed mice over the CPMV-naive mice (median survivals of 91 days over 66 days, $p = 0.0008$) (Figure 3E). These results indicated enhanced potency of the *in situ* vaccine in the presence of pre-existing anti-CPMV antibodies.

Enhanced Phagocytosis of CPMV in the Presence of Antibodies.

We hypothesized that the enhanced efficacy may be explained by pre-existing antibodies enhancing phagocytosis of CPMV based on opsonization, therefore enhancing uptake into innate cells within the tumor microenvironment. We evaluated the influence of anti-CPMV antibodies on phagocytic uptake of CPMV. We compared the phagocytosis of fluorescently tagged CPMV-Cy5/eCPMV-Cy5 particles by bone-marrow-derived macrophages (BMDMs) isolated from C57BL6 mice in the absence or presence of sera from immunized mice; sera from naive mice (no exposure to CPMV) were also used to assess specificity (Figure 4). These studies with macrophages were performed at 37 °C, and therefore cellular uptake of CPMV as opposed to cell binding was expected. BMDMs were gated as the $CD11b^+$ $F4/80^+$ cells, and Cy5 fluorescence intensity derived from the CPMV-Cy5/eCPMV-Cy5 particles was used as a measure of particle uptake (Figure 4A). CPMV particles were readily phagocytosed by BMDMs under all conditions. However, the mean fluorescence intensity (MFI) comparison suggested significantly higher uptake of CPMV in the presence of antisera from immunized mice over bare CPMV and CPMV in the presence of naive sera (~3-fold higher uptake; $p < 0.0001$) (Figure 4B). The same observation was made for eCPMV nanoparticles; here a ~2-fold higher uptake of antisera-coated eCPMV over bare eCPMV was observed (Figure 4C). Similarly, while PEGylation itself reduced phagocytosis of eCPMV particles as expected, preincubation with antisera significantly enhanced uptake, suggesting antibodies were still able to recognize PEG-eCPMV (Figure 4D).

These results indicated that presence of anti-CPMV antibodies could influence the cellular interactions of CPMV/eCPMV particles with immune cells. Since the CPMV immunotherapy acts through interactions with immune cells rather than cancer cells (a key difference from oncolytic viriotherapy), the presence of anti-CPMV antibodies thus enhances the CPMV–immune cell interactions, which likely are the cause for the overserved enhanced antitumor efficacy.

Impact of Pre-existing Antibodies on PEGylated and Native eCPMV *In Situ* Vaccine Efficacy.

We next tested the efficacy of eCPMV *in situ* vaccination; here we tested whether PEGylation had any effect on therapy success using both naive and preimmunized mice. Similar to studies described above, CPMV-naive and CPMV-pre-exposed C57BL6 female mice were challenged with i.p. ID8-Defb/Vegf-a-Luc tumors. Seven days post tumor challenge mice were treated with eCPMV, PEG-eCPMV, or PBS (Figure 5A). Tumor progression was monitored *via* bioluminescence imaging and measurement of weight and circumference. As evident from the bioluminescence imaging, untreated control mice rapidly developed intraperitoneal tumors with wide dissemination throughout the i.p. cavity by day 57 (Figure 5B). Correspondingly, these mice gain significant weight and were euthanized by day 60 (Figure 5C,D). In the CPMV-naive group, eCPMV and

bioluminescence signal from the tumors could be observed as early as day 57, but the weights remained significantly lower than the PBS group. However, by day 61–65 both eCPMV and PEG-eCPMV groups reached the experimental limit of 30 g, whereupon these mice were euthanized (Figure 5C,D). In contrast, the CPMV-pre-exposed group showed significantly reduced tumor burden, as reflected by the minimal bioluminescence signal intensity and smaller changes in mouse weight as late as day 65. In fact, all mice from this group that received eCPMV *in situ* vaccine and 3 out of 5 mice treated with PEG-eCPMV showed minimal disease during the 78-day observation period. Both eCPMV- and PEG-eCPMV-treated mice with pre-existing anti-CPMV antibodies showed a significant survival benefit over CPMV naive mice. These results clearly indicated that presence of pre-existing anti-CPMV antibodies did not diminish, but rather enhanced the efficacy of *in situ* vaccine. No statistically significant difference was observed between eCPMV and PEG-eCPMV treatment in either group, suggesting that PEGylation has no apparent effect on the eCPMV *in situ* vaccine.

We have previously shown that the plant virus CPMV and VLPs thereof are effective *in situ* vaccines. It is evident from our previous studies that multiple administrations of the CPMV *in situ* vaccine are required to overcome immunosuppression and launch systemic antitumor immunity. Because it is well established that viral capsids are immunogenic and will trigger antiviral immune responses,[24] it is imperative to study whether anti-CPMV antibodies are generated during the course of treatment and whether such antibodies are neutralizing efficacy.[26] In this work, we studied the role of anti-CPMV antibodies on *in situ* vaccine efficacy using CPMV and eCPMV as well as PEGylated versions thereof. The free exchange of macromolecules between the plasma and the peritoneal space makes the intraperitoneal ID8 tumor model ideally suited for these studies.[27,28] In particular, it has been demonstrated that the permeability of peritoneal-lining vessels in ascites tumor-bearing animals is greatly increased, which results in a larger influx of macromolecules in the peritoneal cavity from the plasma.[28] Thus, we anticipated draining of the i.p. administered CPMV particles into circulation and lymph nodes priming anti-CPMV immunity and also anticipated integration of anti-CPMV antibodies with i.p. administered CPMV. Throughout the study, subcutaneous immunization was used to mimic prior exposure to CPMV (SET 2) that results in anti-CPMV titers (d −3 sera) equivalent to immunotherapy titers (d 49 sera, SET 1). CPMV immunotherapy led to higher antibody titers over eCPMV and PEG-eCPMV in both naive and pre-exposed mice, validating the stronger immunogenicity of CPMV over eCPMV, likely due to the encapsidated nucleic acid (Figure 2). As a TLR7/8 agonist, viral RNA renders CPMV particles more immunogenic over the capsid-only eCPMV particles (the CPMV capsid signals through TLR2/4) and leads to the elevated antibody titers.[8] Data also confirmed that prior exposure to CPMV leads to a significantly elevated immune response to CPMV, eCPMV, and PEG-eCPMV, which is as expected; the i.p. administrations act as a boost to the initial prime, thus leading to higher antibody titers.

The most interesting data were drawn from the treatment of mice pre-exposed to CPMV; no matter what the therapy was, CPMV *vs* eCPMV *vs* PEGylated eCPMV, the efficacy of the therapy and hence survival of tumor-bearing mice previously exposed to the biologic was significantly enhanced (Figures 3 and 5). The enhanced efficacy could be explained by enhanced immune cell interactions through antibody-mediated opsonization, as was

indicated from macrophage cell uptake studies (Figures 4 and 5). Indeed, the *in situ* vaccine is driven by the interactions of CPMV with resident immune cells in the tumor microenvironment.[18] It should be noted that the presence of antibody is not a prerequisite for the functioning of the CPMV *in situ* vaccine, as demonstrated previously. However, by facilitating enhanced uptake, pre-existing antibodies in CPMV-primed mice are likely contributing to the activation of the local tumor microenvironment and boosting the potency of the *in situ* vaccine. Furthermore, we did not observe any obvious toxicity such as weight loss, respiratory distress, or dermatological reactions from the antibody response in any treatment groups.

Surface passivation strategies based on PEG minimize nanoparticle surface interactions and reduce cellular uptake.[29,30] The impact of PEGylation on the cellular uptake of CPMV by endothelial cells, cancer cells, and immune cells is also well documented.[31–33] While our results mirrored previous studies and indicated significantly reduced phagocytic uptake of PEG-eCPMV over eCPMV by BMDMs in culture (Figure 4C), *in situ* immunotherapy using PEG-eCPMV showed matched efficacy to eCPMV, in naive and CPMV pre-exposed mice, therefore indicating that PEGylation has no effect on the *in situ* vaccine. The cellular uptake of PEGylated nanoparticles, including plant viral nanoparticles, has been shown to be dependent on the PEG grafting density.[34,35] At low PEG densities, the phagocytosis is serum dependent, and adsorption of serum proteins on the particle surfaces significantly enhances cell uptake.[34] Here, the phagocytic uptake of eCPMV and PEG-eCPMV by BMDMs was compared in a serum-free media and the phagocytic uptake of PEG-eCPMV was significantly reduced compared to native eCPMV particles. However, in the presence of sera from immunized mice, increased cellular uptake comparable to native eCPMV was observed (Figure 4D), which mirrors the results from gold nanoparticle uptake studied previously.[34] Furthermore, this enhancement in cell uptake of PEG-eCPMV was only observed in the presence of immunized sera, while the naive sera had no impact on cell uptake, suggesting the influence of anti-CPMV antibodies. While in macrophages, phagocytosis is likely the dominant pathway for nanoparticle uptake, we also acknowledge that CPMV cell entry may be a combination of phagocytosis, endocytosis, and macropinocytosis as previously reported.[36] Thus, the binding of anti-CPMV antibodies could contribute to the enhancement of overall interactions between CPMV and BMDMs through multiple pathways.

Evaluation of CPMV *in situ* vaccine efficacy in the presence of pre-existing antibodies was considered critical given the variable outcomes reported from previous studies involving plant and mammalian viruses under similar scenarios. For example, the efficacy of plant virus papaya mosaic virus (PapMV) as an immune stimulator was completely abrogated upon multiple administrations as measured from the diminished production of IFN-α. The development of this immune tolerance was attributed, in part, to interference from anti-PapMV antibodies.[37] On the contrary, cowpea chlorotic mottle virus (CCMV) carrying RNA replicons showed enhanced uptake and activation of macrophages when preincubated with anti-CCMV antibodies, suggesting improved delivery of the cargo.[38] Thus, the improved efficacy of the CPMV *in situ* vaccine in the presence of pre-existing antibodies is similar to observations made with CCMV and also mirrors the emerging data from oncolytic viruses. For example, in a recent study, pre-existing immunity to Newcastle disease virus (NDV) has been shown to improve its immunotherapeutic efficacy.[39] Several plausible mechanisms

have been suggested including enhanced inflammatory response and recruitment of additional innate and adaptive cells that mediate bystander effect against neighboring cells. Similarly, molecularly retargeted neutralizing antibodies against adenoviruses have been used to further potentiate oncolytic immunotherapy.[40] While CPMV *in situ* vaccine is not dependent on intratumoral replication, there could be some mechanistic overlaps with the enhanced efficacy of oncolytic viruses in the presence of pre-existing antibodies.

CONCLUSIONS

In conclusion, our results demonstrate that pre-existing anti-CPMV antibodies from a prior exposure or a prior treatment do not diminish the efficacy of *in situ* vaccine immunotherapy. On the contrary, pre-existing antibodies could improve the therapeutic efficacy by boosting CPMV–immune cell interactions. These findings carry significant translational implications. They suggest that pre-existing immunity to CPMV should not preclude treatment with CPMV *in situ* vaccine, and repetitive administration of CPMV immunotherapy could actually fuel stronger inflammatory and antitumor responses.

METHODS

Production of CPMV and eCPMV.

CPMV was produced in black-eyed peas (*Vigna unguiculata*) plants using methods described elsewhere. Leaves were inoculated with 100 ng/μL CPMV and harvested after 18–20 days of viral propagation. CPMV was purified from the infected leaves using established methods.[15] Postpurification virus concentration was determined using UV–vis spectroscopy ($\varepsilon_{260\ nm}$ = 8.1 mg^{-1} mL cm^{-1}). eCPMV was produced using agroinfiltration methods described earlier.[16] Briefly, agrobacterium LBA4404 cultures harboring the binary plasmid pEAQexpress-VP60-24K, which encodes coat protein precursor VP60 and viral proteinase 24K, were introduced into *Nicotiana benthamiana* leaves using syringe infiltration. Leaves were harvested 6 days postinfiltration, and eCPMV was purified using established methods. VLP concentration was determined by UV–vis spectroscopy ($\varepsilon_{280\ nm}$ = 1.28 mg^{-1} mL cm^{-1}). Particle integrity was verified using size exclusion chromatography using a Superose6 column on the ÄKTA Explorer chromatography system (GE Healthcare).

Synthesis and Characterization of Fluorescent and PEGylated CPMV.

CPMV-Cy5, eCPMV-Cy5, PEG-eCPMV, and PEG-eCPMV-Cy5 particles were synthesized by covalently conjugating *N*-hydroxysuccinimide-activated esters of Sulfo-Cy5 (NHS-Sulfo-Cy5, Lumiprobe) and PEG2000 (NHS-PEG2000, Nanocs) to the surface-exposed lysine residues on the viral capsid. Briefly, a 5000 molar excess of NHS-Sulfo-Cy5 or NHS-PEG2000 was reacted with CPMV and eCPMV in 0.1 M sodium phosphate (KP) buffer pH 7.4 at a final protein concentration of 2 mg/mL in the presence of 10% (v/v) DMSO for 3 h with constant mixing. CPMV-Cy5/eCPMV-Cy5/PEG-eCPMV particles were purified by ultracentrifugation (133000*g* for 3 h at 4 °C) and resuspended in sterile 0.1 M KP buffer pH 7.4. PEG-eCPMV-Cy5 particles were synthesized by reacting purified eCPMV-Cy5 with NHS-PEG2000 overnight and purifying as above. UV spectroscopy was used to determine

the number of Cy5 dyes/particle using a sulfo-Cy5-specific molar extinction coefficient of ε_{Cy5} of 271 000 L. mol^{-1} cm^{-1} at 647 nm.

SDS-PAGE was used to confirm the degree of PEGylation and confirm covalent attachment of Cy5 to the coat proteins. Briefly, 10 μg of unmodified and dye/PEG-conjugated particles were mixed with SDS running buffer (ThermoFisher Scientific), heated at 100 °C for 5 min, and then loaded on precast NuPAGE 4–12% Bis-Tris protein gels (ThermoFisher Scientific, Waltham, MA, USA); electrophoresis was performed for 40 min at 200 V. Fluorescent bands were visualized on a FluorChem R imager using a 607 nm excitation. The gels were then stained using GelCode Blue Safe protein stain (ThermoFisher Scientific) to visualize the protein bands; the degree of PEGylation was quantified using lane density analysis (ImageJ 1.44o software (Fiji software).

Cell Lines.

The syngeneic ovarian cancer cell line ID8-Defb29/Vegf-a[25] was maintained in RPMI 1640 medium supplemented with 10% (v/v) fetal-bovine serum (FBS) and 1% (v/v) penicillin/streptomycin, 2 mM L-glutamine, 1 mM sodium pyruvate, and 0.05 mM 2-mercaptoethanol at 37 °C and 5% CO_2. The cells were stably transfected with luciferase as described earlier to enable *in vivo* tracking.[41]

BMDM Isolation and Culture.

BMDMs were derived from C57BL6 mice using an established protocol.[42] Briefly, bone marrow was isolated from euthanized mice, and cells were harvested. Following RBC lysis (ACK lysis buffer, ThermoFisher Scientific), cells were cultured in Iscove's modified Eagle's media (ThermoFisher Scientific) supplemented with 10% (v/v) FBS, 2 mM Glutamax, 10 ng mL^{-1} gentamicin, and 10 ng mL^{-1} mouse-colony stimulating factor, M-CSF (Peprotech), for 7–10 days.

Flow Cytometry.

Cellular uptake by BMDMs in the presence or absence of immunized mice sera or naive sera was compared using CPMV-Cy5, eCPMV-Cy5, and PEG-eCPMV-Cy5 particles. Prior to use, BMDMs were removed from M-CSF and resuspended in serum-free DMEM media. CPMV-Cy5, eCPMV-Cy5, or PEG-eCPMV-Cy5 was preincubated with immunized sera or naive sera (1:200 dilutions) or media only (1 μg virus/50 μL serum-free DMEM/well) in a 96-well v-bottom plate at room temperature for 20 min. BMDMs were then added to the wells (200 000 cells/50 μL serum-free DMEM/well), and the plate was incubated at 37 °C and 5% CO_2 for 30 min. Postincubation, cells were washed twice with cold PBS containing 1 mM EDTA and resuspended in staining buffer (PBS with 2% (v/v) FBS, 1 mM EDTA, 0.1% (w/v) sodium azide). Next, Fc receptors were blocked using anti-mouse CD16/CD32 antibody (BioLegend) for 15 min and then stained with fluorescently labeled antibodies FITC-CD11b (clone M1/70) (BioLegend) and PE-F4/80 (clone BM8) (BioLegend) for 30 min on ice. Poststaining cells were washed twice and immediately analyzed using a BD Acuri C6 Plus flow cytometer. Data were analyzed using FlowJo v8.6.3 software.

Mice.

All animal experiments were carried out in accordance with University of California San Diego's Institutional Animal Care and Use Committee. Female C57BL6 mice (7 weeks old) were obtained from Jackson Lab.

Immunizations.

Mice were immunized twice in a 14-day period with 50 μg of CPMV/eCPMV or PEG-eCPMV in sterile PBS using subcutaneous injections. Blood was collected *via* retro-orbital bleeding in Greiner Bio-One Vacuette MiniCollect tubes (ThermoFisher Scientific). Serum was separated and stored at 4 °C until analyzed.

Antibody Titers and Isotypes.

Following immunizations, ELISAs were carried out to determine CPMV-specific IgG titers and IgG isotypes. Nunc Polysorp Immuno plates (96-well, ThermoFisher Scientific) were coated with 2 μg of CPMV in coating buffer (0.1 M sodium phosphate, 0.15 M sodium chloride, 10 mM EDTA, pH 7.2) and incubated overnight at 4 °C. Plates were washed three times with washing buffer (0.05% (v/v) Tween-20 in PBS, 200 μL per well) after coating and between all subsequent steps. Following blocking with 100 μL of blocking solution (2.5% dry milk, 25% FBS in PBS) for an hour, sera from immunized mice were added to the wells using a dilution series (in blocking buffer), and plates were incubated for 2 h at 37 °C. Next, plates were incubated with 100 μL of alkaline phosphatase-labeled goat anti-mouse IgG (Invitrogen, ThermoFisher Scientific) in blocking buffer (at 1:1000 dilution) at 37 °C for 1 h and developed with 100 μL of 1-step PNPP substrate (ThermoFisher Scientific) for 10 min at 4 °C. Reaction was stopped using 50 μL of 2 M NaOH. Absorbance was then read at 405 nm using a Tecan microplate reader. For IgG isotyping, anti-mouse IgG2a, IgG2b, IgG1, and IgM-alkaline phosphatase antibodies were used as the secondary antibodies (Biolegend) at 1:1000 dilutions. Plates were then developed using PNPP substrate, and absorbance was measured as described above.

Tumor Challenge, Monitoring, and *In Situ* Vaccine Immunotherapy.

A 2×10^6 amount of live ID8-Defb29/Vegf-a or ID8-Defb29/Vegf-a-Luc cells/200 μL PBS was orthotopically implanted into mice by i.p. injections. Mice were monitored weekly for signs of tumor progression, including abdominal distension, weight, and circumference. Tumor growth was also monitored using bioluminescence imaging in mice injected with ID8-Defb29/Vegf-a-Luc cells. Mice were i.p. injected with luciferin (150 mg/kg, Thermo Scientific Pierce) and imaged in an IVIS Spectrum Imaging System (PerkinElmer Ltd.). Total bioluminescence was determined using Living Image software (PerkinElmer Ltd.). Regions of interest were quantified as average radiance (photons/s). Mice were euthanized when weight reached 30 g or circumference reached 10 cm or when moribund.

CPMV naive ($n = 9$) or CPMV pre-exposed mice ($n = 10$) inoculated with ID8-Defb29/Vegf-a tumors were treated with six weekly doses of CPMV *via* i.p. injections (100 μg in 200 μL of PBS) starting at 7 days from tumor challenge, and tumor progression was compared to PBS (200 μL)-treated mice ($n = 6$). Similarly, naive or CPMV pre-exposed mice inoculated with bioluminescent ID8-Defb29/Vegf-a-Luc tumors were treated with six

weekly doses of 100 μg of eCPMV (n = 5 each of CPMV naive and CPMV pre-exposed mice) or PEG-eCPMV (n = 5 each of CPMV naive and CPMV pre-exposed mice) *via* i.p. injections and compared to PBS-treated (n = 5) mice for tumor progression as described above. Mice were euthanized when the weight reached 30 g or the circumference reached 10 cm or when moribund.

ACKNOWLEDGMENTS

This work was supported in part by a grant from the NCI Alliance for Nanotechnology in Cancer U01CA218292 and NCI grant R01CA224605 (to N.F.S.).

REFERENCES

(1). Rosenberg SA Decade in Review-Cancer Immunotherapy: Entering the Mainstream of Cancer Treatment. Nat. Rev. Clin. Oncol 2014, 11, 630–632. [PubMed: 25311350]

(2). Joyce JA; Fearon DT T Cell Exclusion, Immune Privilege, and the Tumor Microenvironment. Science 2015, 348, 74–80. [PubMed: 25838376]

(3). Goto T Radiation as an In Situ Auto-Vaccination: Current Perspectives and Challenges. Vaccines (Basel, Switz.) 2019, 7, 100.

(4). Le QV; Suh J; Choi JJ; Park GT; Lee JW; Shim G; Oh YK *In Situ* Nanoadjuvant-Assembled Tumor Vaccine for Preventing Long-Term Recurrence. ACS Nano 2019, 13, 7442–7462. [PubMed: 31180642]

(5). Bommareddy PK; Kaufman HL Unleashing the Therapeutic Potential of Oncolytic Viruses. J. Clin. Invest 2018, 128, 1258–1260. [PubMed: 29504947]

(6). Lizotte PH; Wen AM; Sheen MR; Fields J; Rojanasopondist P; Steinmetz NF; Fiering S *In Situ* Vaccination with Cowpea Mosaic Virus Nanoparticles Suppresses Metastatic Cancer. Nat. Nanotechnol 2016, 11, 295–303. [PubMed: 26689376]

(7). Murray AA; Wang C; Fiering S; Steinmetz NF *In Situ* Vaccination with Cowpea *vs* Tobacco Mosaic Virus against Melanoma. Mol. Pharmaceutics 2018, 15, 3700–3716.

(8). Wang C; Beiss V; Steinmetz NF Cowpea Mosaic Virus Nanoparticles and Empty Virus-Like Particles Show Distinct but Overlapping Immunostimulatory Properties. J. Virol 2019, 93, No. e00129–19. [PubMed: 31375592]

(9). Kerstetter-Fogle A; Shukla S; Wang C; Beiss V; Harris PLR; Sloan AE; Steinmetz NF Plant Virus-Like Particle *In Situ* Vaccine for Intracranial Glioma Immunotherapy. Cancers 2019, 11, No. e515. [PubMed: 30974896]

(10). Hoopes PJ; Wagner RJ; Duval K; Kang K; Gladstone DJ; Moodie KL; Crary-Burney M; Ariaspulido H; Veliz FA; Steinmetz NF; Fiering SN Treatment of Canine Oral Melanoma with Nanotechnology-Based Immunotherapy and Radiation. Mol. Pharmaceutics 2018, 15, 3717–3722.

(11). Kawai T; Akira S The Role of Pattern-Recognition Receptors in Innate Immunity: Update on Toll-Like Receptors. Nat. Immunol 2010, 11, 373–384. [PubMed: 20404851]

(12). VanBlargan LA; Goo L; Pierson TC Deconstructing the Antiviral Neutralizing-Antibody Response: Implications for Vaccine Development and Immunity. Microbiol. Mol. Biol. Rev 2016, 80, 989–1010. [PubMed: 27784796]

(13). Liu R; Vaishnav RA; Roberts AM; Friedland RP Humans Have Antibodies Against a Plant Virus: Evidence from Tobacco Mosaic Virus. PLoS One 2013, 8, No. e60621. [PubMed: 23573274]

(14). Colson P; Richet H; Desnues C; Balique F; Moal V; Grob JJ; Berbis P; Lecoq H; Harle JR; Berland Y; Raoult D Pepper Mild Mottle Virus, a Plant Virus Associated with Specific Immune Responses, Fever, Abdominal Pains, and Pruritus in Humans. PLoS One 2010, 5, No. e10041. [PubMed: 20386604]

(15). Wellink J Comovirus Isolation and RNA Extraction. Methods Mol. Biol 1998, 81, 205–209. [PubMed: 9760508]

(16). Saunders K; Sainsbury F; Lomonossoff GP Efficient Generation of Cowpea Mosaic Virus Empty Virus-Like Particles by the Proteolytic Processing of Precursors in Insect Cells and Plants. Virology 2009, 393, 329–337. [PubMed: 19733890]

(17). Chatterji A; Ochoa WF; Paine M; Ratna BR; Johnson JE; Lin T New Addresses on an Addressable Virus Nanoblock; Uniquely Reactive Lys Residues on Cowpea Mosaic Virus. Chem. Biol 2004, 11, 855–863. [PubMed: 15217618]

(18). Wang C; Fiering SN; Steinmetz NF Cowpea Mosaic Virus Promotes Anti-Tumor Activity and Immune Memory in a Mouse Ovarian Tumor Model. Advanced Therapeutics 2019, 2, 1900003.

(19). Guan C; Chernyak N; Dominguez D; Cole L; Zhang B; Mirkin CA RNA-Based Immunostimulatory Liposomal Spherical Nucleic Acids as Potent TLR7/8 Modulators. Small 2018, 14, No. e1803284. [PubMed: 30370991]

(20). Komura F; Takahashi Y; Inoue T; Takakura Y; Nishikawa M Development of a Nanostructured RNA/DNA Assembly as an Adjuvant Targeting Toll-Like Receptor 7/8. Nucleic Acid Ther. 2019, 29, 335–342. [PubMed: 31329033]

(21). Madan-Lala R; Pradhan P; Roy K Combinatorial Delivery of Dual and Triple TLR Agonists *via* Polymeric Pathogen-Like Particles Synergistically Enhances Innate and Adaptive Immune Responses. Sci. Rep 2017, 7, 2530. [PubMed: 28566683]

(22). Lebel ME; Chartrand K; Tarrab E; Savard P; Leclerc D; Lamarre A Potentiating Cancer Immunotherapy Using Papaya Mosaic Virus-Derived Nanoparticles. Nano Lett. 2016, 16, 1826–1832. [PubMed: 26891174]

(23). Cai H; Shukla S; Wang C; Masarapu H; Steinmetz NF Heterologous Prime-Boost Enhances the Antitumor Immune Response Elicited by Plant-Virus-Based Cancer Vaccine. J. Am. Chem. Soc 2019, 141, 6509–6518. [PubMed: 30995022]

(24). Shukla S; Myers JT; Woods SE; Gong X; Czapar AE; Commandeur U; Huang AY; Levine AD; Steinmetz NF Plant Viral Nanoparticles-Based HER2 Vaccine: Immune Response Influenced by Differential Transport, Localization and Cellular Interactions of Particulate Carriers. Biomaterials 2017, 121, 15–27. [PubMed: 28063980]

(25). Conejo-Garcia JR; Benencia F; Courreges MC; Kang E; Mohamed-Hadley A; Buckanovich RJ; Holtz DO; Jenkins A; Na H; Zhang L; Wagner DS; Katsaros D; Caroll R; Coukos G Tumor-Infiltrating Dendritic Cell Precursors Recruited by a Beta-Defensin Contribute to Vasculogenesis Under the Influence of Vegf-A. Nat. Med 2004, 10, 950–958. [PubMed: 15334073]

(26). Ferguson MS; Lemoine NR; Wang Y Systemic Delivery of Oncolytic Viruses: Hopes and Hurdles. Adv. Virol 2012, 2012, 805629. [PubMed: 22400027]

(27). Flessner MF; Dedrick RL; Schultz JS Exchange of Macromolecules between Peritoneal Cavity and Plasma. Am. J. Physiol 1985, 248, H15–25. [PubMed: 2578740]

(28). Nagy JA; Herzberg KT; Masse EM; Zientara GP; Dvorak HF Exchange of Macromolecules between Plasma and Peritoneal Cavity in Ascites Tumor-Bearing, Normal, and Serotonin-Injected Mice. Cancer Res. 1989, 49, 5448–5458. [PubMed: 2475250]

(29). Jokerst JV; Lobovkina T; Zare RN; Gambhir SS Nanoparticle Pegylation for Imaging and Therapy. Nanomedicine (London, U. K.) 2011, 6, 715–728. [PubMed: 21718180]

(30). Qie Y; Yuan H; von Roemeling CA; Chen Y; Liu X; Shih KD; Knight JA; Tun HW; Wharen RE; Jiang W; Kim BY Surface Modification of Nanoparticles Enables Selective Evasion of Phagocytic Clearance by Distinct Macrophage Phenotypes. Sci. Rep 2016, 6, 26269. [PubMed: 27197045]

(31). Gonzalez MJ; Plummer EM; Rae CS; Manchester M Interaction of Cowpea Mosaic Virus (CPMV) Nanoparticles with Antigen Presenting Cells *In Vitro* and *In Vivo*. PLoS One 2009, 4, No. e7981. [PubMed: 19956734]

(32). Lewis JD; Destito G; Zijlstra A; Gonzalez MJ; Quigley JP; Manchester M; Stuhlmann H Viral Nanoparticles as Tools for Intravital Vascular Imaging. Nat. Med 2006, 12, 354–360. [PubMed: 16501571]

(33). Steinmetz NF; Manchester M Pegylated Viral Nanoparticles for Biomedicine: The Impact of PEG Chain Length on VNP Cell Interactions *In Vitro* and *Ex Vivo*. Biomacromolecules 2009, 10, 784–792. [PubMed: 19281149]

(34). Walkey CD; Olsen JB; Guo H; Emili A; Chan WC Nanoparticle Size and Surface Chemistry Determine Serum Protein Adsorption and Macrophage Uptake. J. Am. Chem. Soc 2012, 134, 2139–2147. [PubMed: 22191645]

(35). Lee KL; Shukla S; Wu M; Ayat NR; El Sanadi CE; Wen AM; Edelbrock JF; Pokorski JK; Commandeur U; Dubyak GR; Steinmetz NF Stealth Filaments: Polymer Chain Length and Conformation Affect the *In Vivo* Fate of Pegylated Potato Virus X. Acta Biomater. 2015, 19, 166–179. [PubMed: 25769228]

(36). Plummer EM; Manchester M Endocytic Uptake Pathways Utilized by CPMV Nanoparticles. Mol. Pharmaceutics 2013, 10, 26–32.

(37). Chartrand K; Lebel ME; Tarrab E; Savard P; Leclerc D; Lamarre A Efficacy of a Virus-Like Nanoparticle as Treatment for a Chronic Viral Infection is Hindered by IRAK1 Regulation and Antibody Interference. Front. Immunol 2018, 8, 1885. [PubMed: 29354118]

(38). Biddlecome A; Habte HH; McGrath KM; Sambanthamoorthy S; Wurm M; Sykora MM; Knobler CM; Lorenz IC; Lasaro M; Elbers K; Gelbart WM Delivery of Self-Amplifying RNA Vaccines in *In Vitro* Reconstituted Virus-Like Particles. PLoS One 2019, 14, No. e0215031. [PubMed: 31163034]

(39). Ricca JM; Oseledchyk A; Walther T; Liu C; Mangarin L; Merghoub T; Wolchok JD; Zamarin D Pre-Existing Immunity to Oncolytic Virus Potentiates Its Immunotherapeutic Efficacy. Mol. Ther 2018, 26, 1008–1019. [PubMed: 29478729]

(40). Niemann J; Woller N; Brooks J; Fleischmann-Mundt B; Martin NT; Kloos A; Knocke S; Ernst AM; Manns MP; Kubicka S; Wirth TC; Gerardy-Schahn R; Kuhnel F Molecular Retargeting of Antibodies Converts Immune Defense against Oncolytic Viruses into Cancer Immunotherapy. Nat. Commun 2019, 10, 3236. [PubMed: 31324774]

(41). Patel R; Czapar AE; Fiering S; Oleinick NL; Steinmetz NF Radiation Therapy Combined with Cowpea Mosaic Virus Nanoparticle *In Situ* Vaccination Initiates Immune-Mediated Tumor Regression. ACS Omega 2018, 3, 3702–3707. [PubMed: 29732445]

(42). Liu M; O'Connor RS; Trefely S; Graham K; Snyder NW; Beatty GL Metabolic Rewiring of Macrophages by CpG Potentiates Clearance of Cancer Cells and Overcomes Tumor-Expressed CD47-Mediated 'Don't-Eat-Me' Signal. Nat. Immunol 2019, 20, 265–275. [PubMed: 30664738]

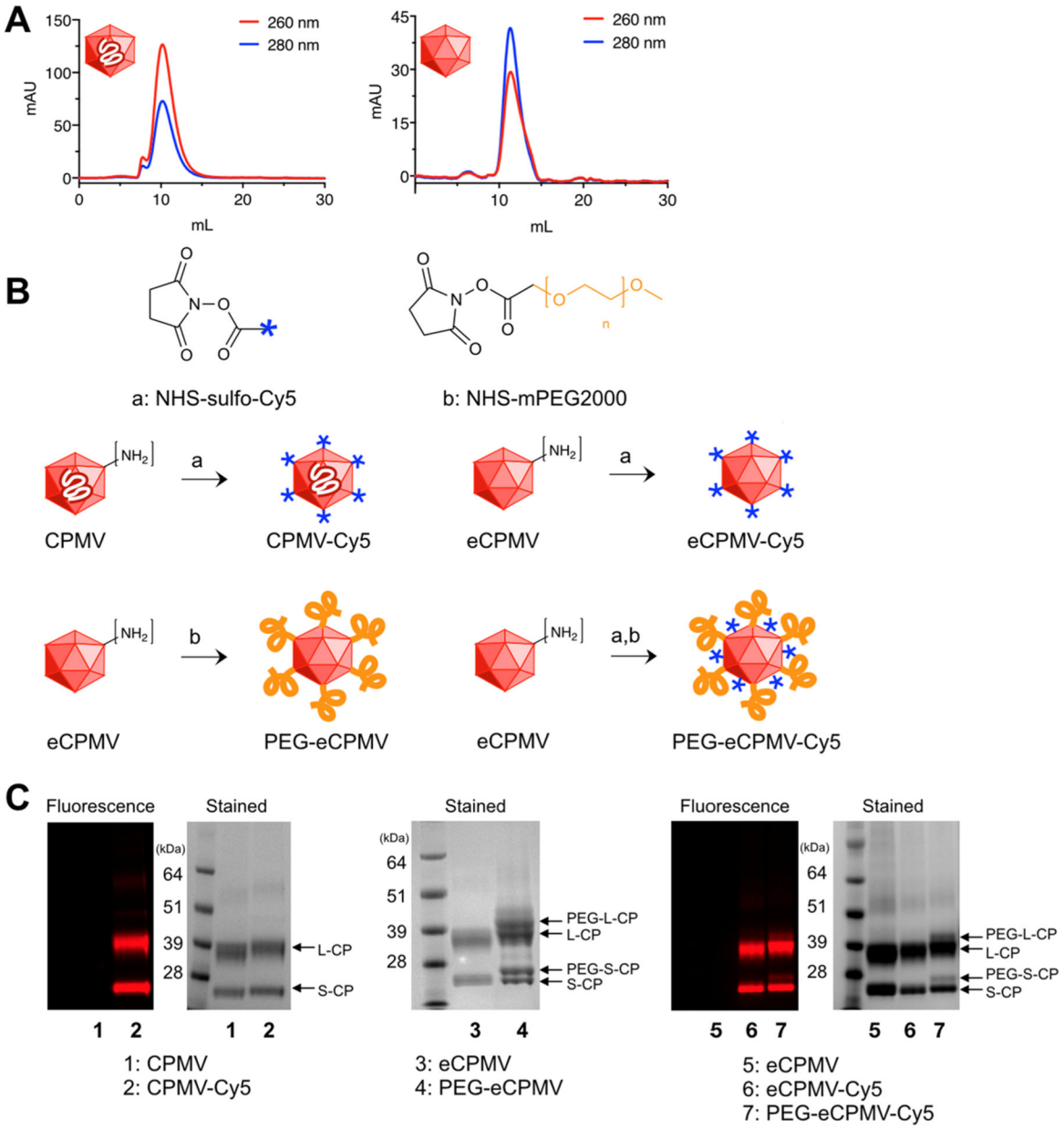

Figure 1.

Bioconjugation and characterization of CPMV and eCPMV particles. CPMV and eCPMV were propagated in plants. Postpurification, particle integrity was determined using size exclusion chromatography (A); *N*-hydroxysuccinimide (NHS) chemistry was used to conjugate fluorescent dye Sulfo-Cy5 and/or PEG2000 to the (e) CPMV coat proteins *via* the lysine residues to obtain CPMV-Cy5, eCPMV-Cy5, PEG-eCPMV, and PEG-eCPMV-Cy5 (B). SDS-PAGE (4–12% NuPAGE gel) gels were imaged on a FluorChem R imager, first using the MultiFluor Red channel under 607 nm excitation (fluorescence image) to verify dye conjugation and then stained with GelCode Blue Safe protein stain and visualized under white light (stained image). Stained gel image was used to verify and quantify covalent conjugation of PEG molecules to the small (S) and large (L) coat proteins (CP) of eCPMV.

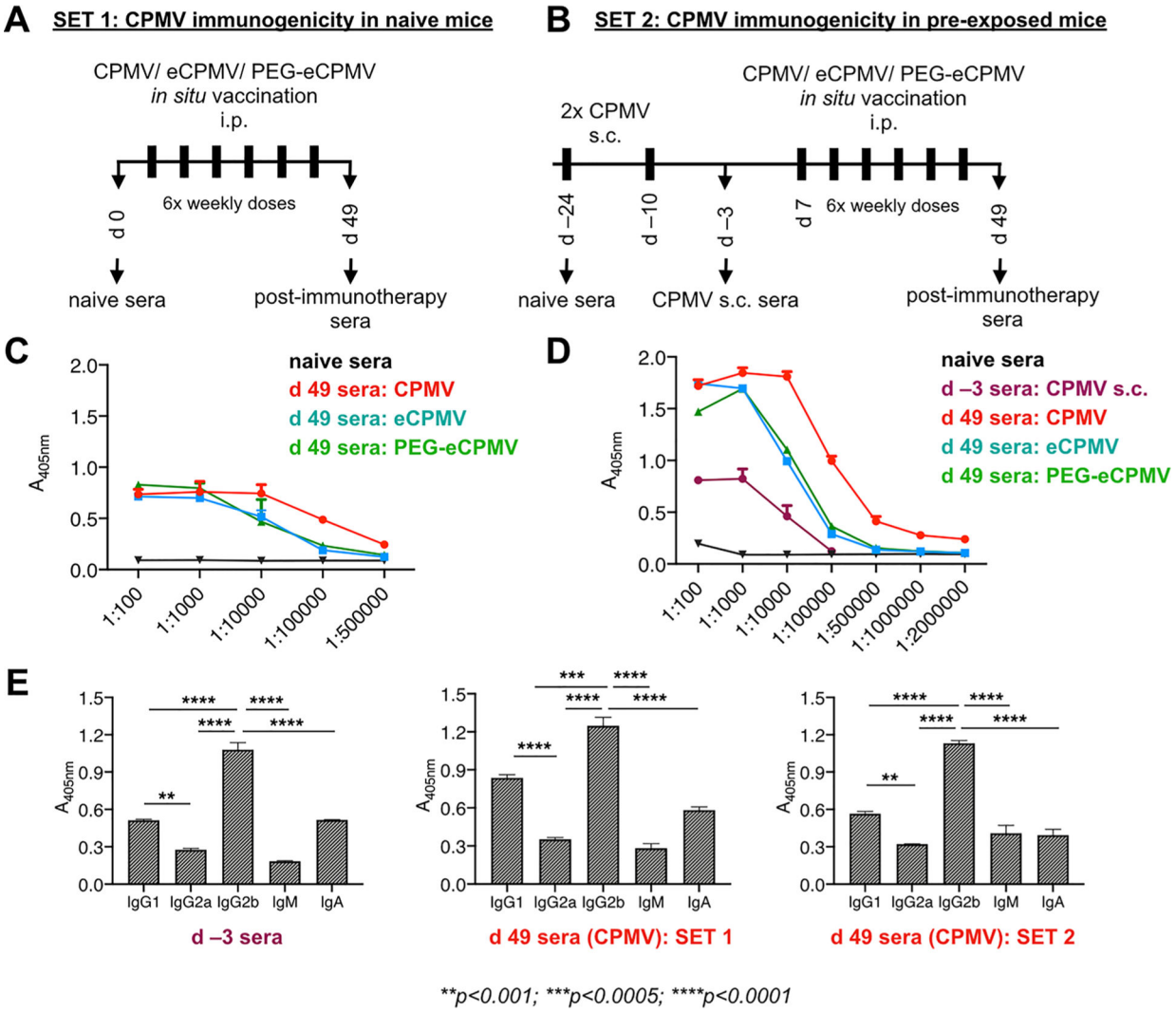

Figure 2.

Immunogenicity of CPMV, eCPMV, and PEG-eCPMV leads to generation of anti-CPMV antibodies. Immunogenicity of intraperitoneal (i.p.) administered CPMV, eCPMV, and PEG-eCPMV was evaluated in CPMV naive (SET 1) or preimmunized (SET 2) C57BL6 female mice; mice received 6 weekly i.p. doses to mimic the typical administration schedule for i.p. *in situ* vaccines (A, B). Anti-CPMV antibody titers (C, D) and isotypes (E) were measured using ELISAs performed on CPMV-coated plates. Statistical analysis was performed by ordinary one-way ANOVA and Tukey's multiple comparisons test using GraphPad Prism software.

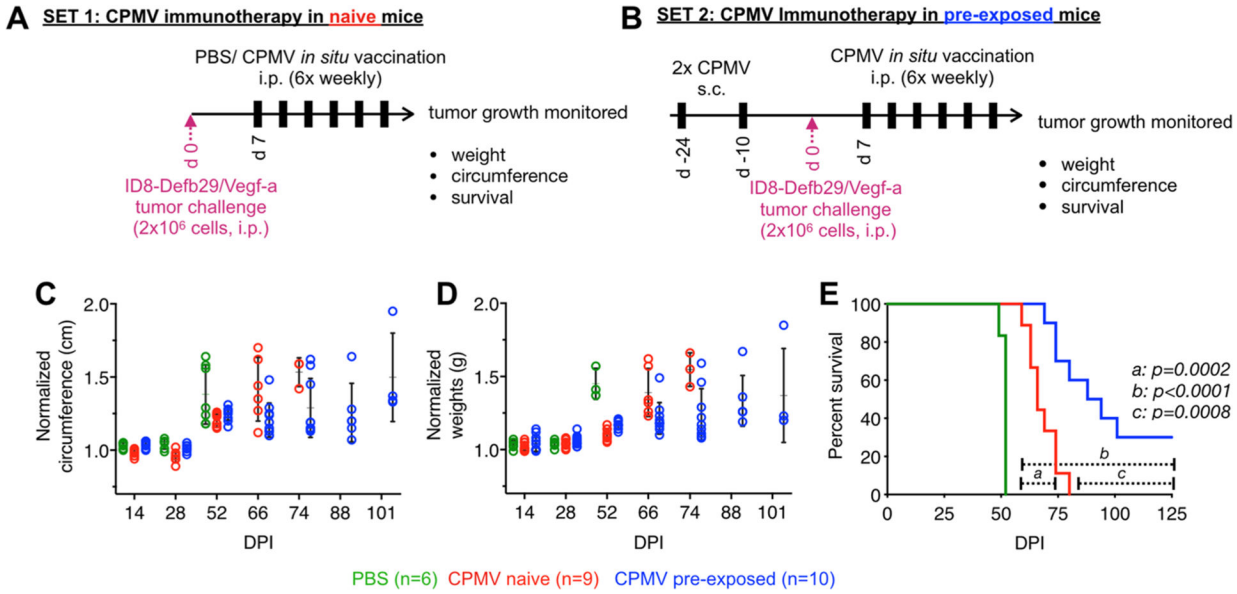

Figure 3.

Pre-exposure to CPMV improves efficacy of CPMV *in situ* vaccine in ID8-Defb29/Vegf-a ovarian tumors. Efficacy of CPMV *in situ* vaccination (100 μg in 200 μL of PBS) against i.p. established ID8-Defb29/Vegf-a ovarian tumors in female C57BL6 mice was tested in CPMV-naive *vs* CPMV-pre-exposed mice (A, B). Tumor progression was monitored by measuring gains in circumference (C) and body weight (D). Survival was monitored for 125 days (E). Kaplan–Meier plots were used to compare survival between groups. Statistical analysis on the survival curves was performed using the log-rank (Mantel–Cox) test using GraphPad Prism 8 software.

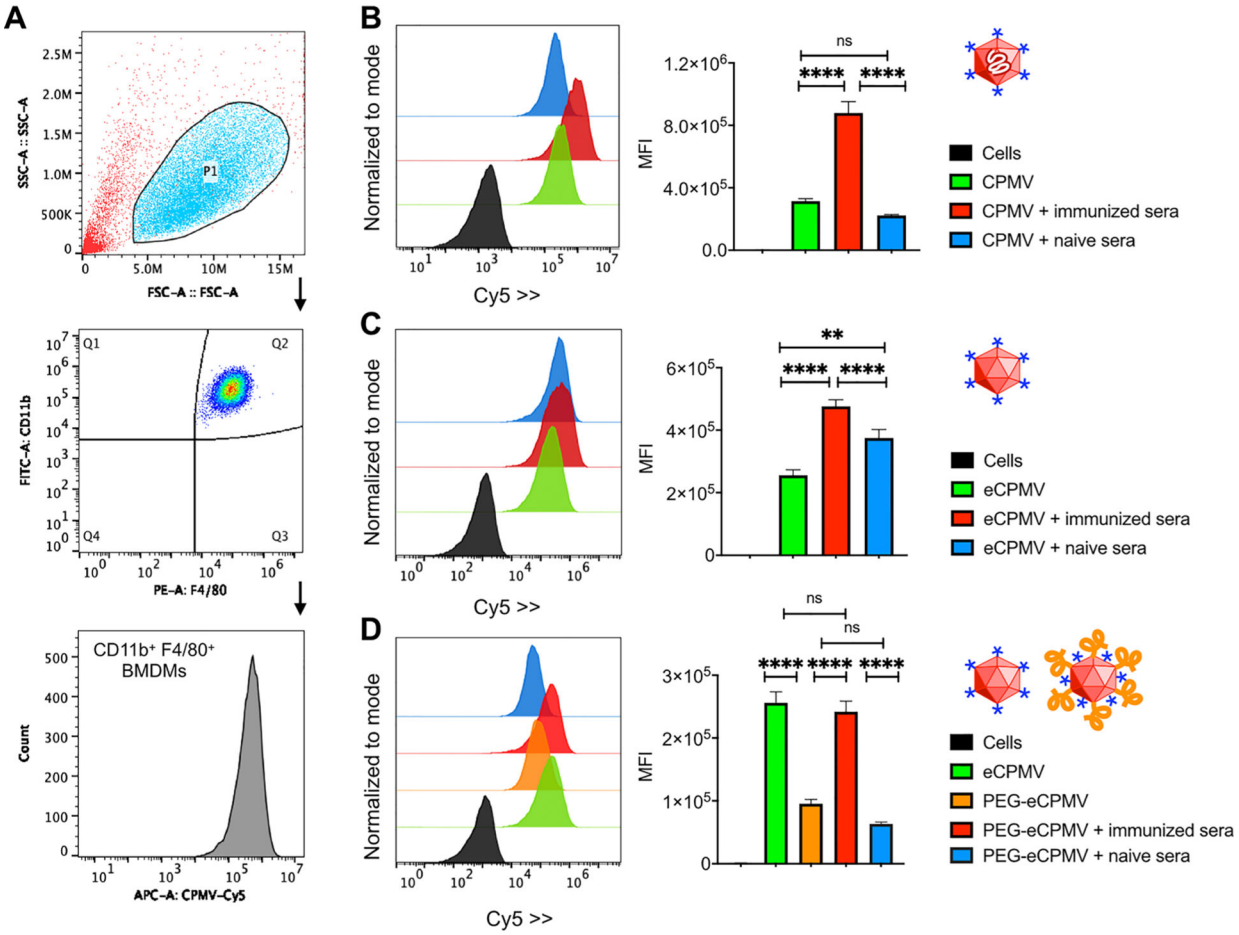

Figure 4.

Anti-CPMV antibodies enhance the phagocytic uptake of CPMV, eCPMV, and PEG-eCPMV by bone-marrow-derived macrophages (BMDMs). BMDMs cultured for 10 days in the presence of M-CSF were gated as $CD11b^+$ $F4/80^+$ cells. Phagocytic uptake of Cy5-labeled CPMV, eCPMV, and PEG-eCPMV was compared using flow cytometry in the absence and presence of day 49 sera (immunized sera) from CPMV-pre-exposed mice and sera from naive mice (naive sera) (B, C, and D). Particles (1 μg) were pre-exposed to sera (1:200 dilutions) for 20 min and subsequently incubated with 200 000 BMDMs for 30 min. Cell uptake was analyzed using flow cytometry. Statistical analysis was performed using ordinary one-way ANOVA–Tukey's multiple comparisons test (****$p < 0.0001$; **$p = 0.0048$).

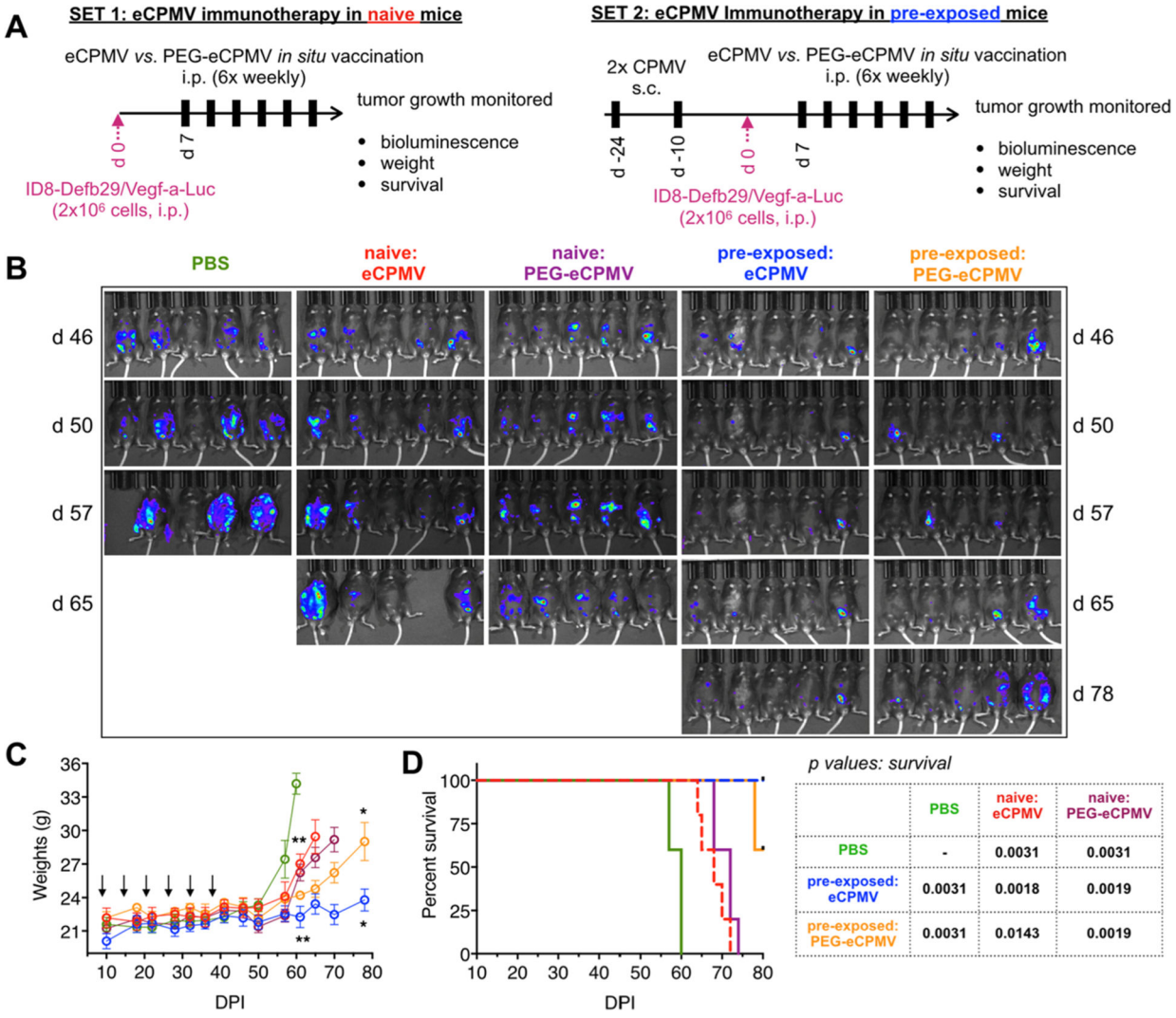

Figure 5.

eCPMV and PEG-eCPMV *in situ* vaccines display improved efficacy against ID8-Defb29/Vegf-a-Luc ovarian tumors in CPMV pre-exposed mice. The efficacy of eCPMV and PEG-eCPMV was tested in CPMV-naive and CPMV-pre-exposed female C57BL6 mice challenged i.p. with bioluminescent ID8-Defb29/Vegf-a-Luc ovarian cancer cells (A). Tumor progression was monitored using bioluminescence imaging (B), body weight (C), and survival (D); color scheme in C and D: PBS, green; naive eCPMV, red; naive PEG-eCPMV, purple; pre-exposed/eCPMV, blue; pre-exposed/PEG-eCPMV, orange. Statistical analysis was performed using unpaired *t* test for weights (d61: eCPMV naive *vs* pre-exposed $^{**}p = 0.006$; PEG-eCPMV naive *vs* pre-exposed $^{**}p = 0.03$; d78: eCPMV naive *vs* pre-exposed $^{*}p = 0.02$); survival curves were compared by log-rank (Mantel–Cox) test using GraphPad Prism 8 software.